Characterization of amorphous hydrocarbon CD_x films ($x \sim 0.5$) for energy storage applications

Maria Brzhezinskaya[a], Nikolay Yu. Svechnikov[b]*, Vladimir G. Stankevich[b], Alexei M. Lebedev[b], Leonid P. Sukhanov[b,c], and Konstantin A. Menshikov[b]

[a]*Main Department Scientific-Technical Infrastructure II, Helmholtz-Zentrum Berlin für Materialien und Energie, 12489 Berlin, Germany;*

[b]*Laboratory of Synchrotron-Neutron Research, National Research Centre Kurchatov Institute, 123182 Moscow, Russia*

[c]*Department of Theoretical Physics, Moscow Institute of Physics and Technology, 141700 Dolgoprudny, Russia*

*Corresponding author:
Dr. habil. Nikolai Yu. Svechnikov
National Research Centre Kurchatov Institute,
Academician Kurchatov Square 1, 123182 Moscow, Russia
E-mail: svechnikov47@mail.ru

Characterization of amorphous hydrocarbon CD_x films ($x \sim 0.5$) for energy storage applications

Smooth hydrocarbon films formed on the vacuum chamber walls in tokamaks under the erosion of graphite elements during deuterium plasma discharges are the main accumulators of hydrogen isotopes in carbon matrices. Therefore, they can be considered as a promising material for hydrogen storage applications. In the present work, such hydrocarbon CD_x films (x~0.5) produced in T-10 tokamak (NRC Kurchatov Institute, Russia) were studied using scanning electron microscopy (SEM), NEXAFS and EXAFS spectroscopies together with thermal desorption (TD) for the films' characterization and estimation of their hydrogen storage capacity.
The C 1*s* X-ray absorption spectra of the CD_x films were recorded for the first time using the BESSY II storage ring facility (Germany). The obtained NEXAFS spectra were found typical for CK-spectra of $sp^3 + sp^2$ hydrocarbon systems with a high H/C ratio. The role of Fe impurities from the tokamak chamber walls was elucidated as a catalytic effect "facilitating" the thermal desorption of hydrogen (deuterium) from CD_x films. The Fe *K*-edge spectra allowed to confirm a fractal (self-affined) structure of CD_x films, with a minimal sp^2 fractal aggregate ~2–3 nm, and formation of 3*D* carbon sp^3+sp^2 network, accumulated a large number of H-isotopes and C_xH_y hydrocarbons. It was found that the H storage and thermal desorption properties of the CD_x films can be improved by their inherent Fe impurities, capable to reduce the barrier of TD and to increase the H/C storage capacity by several times even at room temperature.

Keywords: Amorphous hydrocarbon films, high hydrogen content, X-ray absorption spectroscopy, Fe catalytic effect, hydrogen storage

Introduction

Hydrogen is one of the most promising materials for energy storage and transportation, since its reserves are almost inexhaustible, and its use does not threaten the ecology of our planet. Carbon nanomaterials, due to their low density, high specific surface, porosity, thermal and chemical stability, are considered among the most promising materials for hydrogen storage. Among them, carbon nanotubes, graphitic nanofibers and mechanically milled graphite, have attracted a large attention over the past decades as hydrogen storage materials [1]. It is also worth mentioning the creation of highly efficient hydrogen energy carbon matrices based on typical tokamak carbon films with high hydrogen (deuterium) content. For example, in the case of amorphous CD_x films ($x \sim 0.5$, 20 – 30 μm thick) deposited on the vacuum chamber walls at a wall temperature of 300 – 400 K under the erosion of graphite elements of the T-10 tokamak (NRC Kurchatov Institute, Moscow) during D-plasma discharges [2].

Important to note that the thermal desorption (TD) D_2 curve of CD_x films within the 400 – 1000 K range [3] appeared to be comparable to that for a nanostructured graphite powder mechanically milled under hydrogen atmosphere of 1 MPa made by Orimo [4] and showed a hydrogen sorption capacity of 6 mass%. This fact together with the observed similarities in XRD and Raman spectra show the similarities in the TD processes in both systems, and two main adsorption states of hydrogen isotopes were found for CD_x films [3]. Moreover, these hydrocarbon films are the main accumulator of hydrogen isotopes in tokamaks. Not only hydrogen isotopes, but also, hydrocarbon radicals (consisting of D, H components) of C_1 - group (CH_n, n =1 – 3), C_2 - group (C_2H_n, n = 1 – 5) and C_3- group (C_3H_n), may be effused during thermal desorption at temperatures lower than those of H_2 and D_2 hydrogens.

In this work, the recorded CK-spectra of CD_x films were typical for XAS spectra of K-shells of sp^3+sp^2 hydrocarbon systems with high hydrogen content and a high sp^3 ratio. This agrees with a fractal structure of CD_x films [2], forming a branched and highly cross-linked 3-dimentional carbon sp^3+sp^2 network, accumulating a large number of H-isotopes and hydrocarbons of C_1 – C_3 families, which storage and thermal desorption properties can be improved by their inherent Fe impurities (<1 at.%) originating from chamber walls erosion during plasma discharges [5].

The Fe impurity in CD_x films was discovered by means of X-ray fluorescence (XRFA–SR), extended X-ray absorption fine structure (EXAFS) at the *K* absorption edge of iron, electron paramagnetic resonance (EPR) (wide line with *g* ~2.1), as well as with the help of X-ray diffraction and X-ray photoelectron spectroscopy [5, 6, 7].

All these features of CD_x films will contribute to the energy applications of these unique and still insufficiently studied hydrocarbon storage systems.

Materials and methods

Sample preparation, thermogravimetric analysis and thermal desorption

During tokamak operation its plasma facing components, i.e., limiter and annular diaphragm made of a fine grain graphite MPG-8, intended for central plasma region confinement and chamber wall protection against heat load and plasma disruptions, are exposed to physical and chemical sputtering. The amorphous homogeneous CD_x films with a high D/C (H/C) ratio used in this work, were deposited out of “direct vision” of central deuterium plasma, as a result of erosion and redeposition on the T-10 tokamak vacuum chamber walls under multiple action of both plasma working and cleaning (of low-temperature plasma) discharges. The main plasma parameters involved in the formation of these films were the following: toroidal field 2.8 T, electron temperature of core plasma – up to 1 keV, ion temperature 450–700 eV, ion plasma current 250–300 kA, electron density $(2–3)\cdot 10^{19}$ m^{-3}, working discharge duration – 1 s (above 1000 working discharges for producing thick films and 1000 hours of cleaning discharges).

The Rutherford backscattering in combination with the resonance elastic scattering was used for analysis of deposits composition H/C and D/C [3].

The maximal H/C atomic ratio can rise to a value of ~1–2 for samples with high *sp*^{3} values. After reaching the thicknesses of 20–30 μm, these “flakes”, experiencing internal stress, peel off from the chamber walls and fall down in a form of free standing flakes (Fig. 1). Here, surface defects formed by exposure to plasma ions, electrons and neutrals act as hydrogen trapping sites, forming pores and blisters (Fig. 1). The hydrogen sorption capacity of CD_x films, formed by plasma particles, will be additionally increased due to opening of micropores under moderate heating, namely up to 4 times at 620 K for outgassing fraction (relative mass loss) of 14% [8].

According to our thermogravimetric data [8] and results from Yin [9] for as-prepared a-C:H films with a high *sp*^{3} ratio (as in CD_x films), the appropriate value of specific surface area (BET) equals at least 200 m^{2}g^{-1}, as follows from the typical dependence of the BET surface area and porosity versus the outgassing fraction. It is obvious that a large fraction of *sp*^{3} bonds in the CD_x structure and high internal stress impede more intense porosity formation at room temperature, i.e. before heating.

As we reported earlier, the thermal desorption (TD) D_2 curve of CD_x films [3] is comparable to that observed by Orimo [4] for a mechanically milled nanostructured graphite powder, and both TD were measured under the same heating rate 10 K/min. Orimo [4] used a planetary ball mill apparatus (with steel balls) during milling under hydrogen atmosphere of 1 MPa at room temperature for 80 hours, i.e. up to graphite crystallite sizes <4 nm, with a sorption capacity of 6 mass% of hydrogen (as a mixture of pure hydrogen and hydrocarbons in TD spectra, despite a low BET area of 10 m^{2}g^{-1} at room temperature). The TD curves for $D_2(H_2)$ [3] consist of two groups of peaks, a broad one at 450–800 K with a maximum near 750 K (including hydrogen and hydrocarbons, the latter desorb up to ~700 K), and a narrow asymmetric one at 900–1000 K with a maximum at 970 K. This TD resemblance together with the observed similarities in XRD and Raman spectra show the similarities in the TD processes occurring in both systems within the given temperature range. Also, the minimum achieved graphite sp^2 crystallite sizes below 4 nm of Orimo [4] appeared to be rather close in size to the minimal sp^2 fractal aggregate ~2–3 nm, consisting of three benzene rings in a fractal model of CD_x films [2]. Therefore, the reported data on activation energies were used for interpretation of TD spectra of CD_x films, showing two main adsorption states of hydrogen isotopes: a weak ”physisorbed” state with a binding energy per atom ~0.65 eV/H and a strong chemisorbed state with a binding energy ~1.25 eV/H [3].

NEXAFS and EXAFS spectroscopies

C 1*s* X-ray absorption spectra were measured for CD_x films at the Russian–German beamline of the BESSY II storage ring of Helmholtz-Zentrum Berlin (Berlin, Germany) in the total electron yield (TEY) mode [10]. The thick free standing CD_x flakes (20 – 30 μm thick) were pressed into the indium foil to reduce the effect of surface charging. The measurements were performed at the photon energies of $h\nu$=275–330 eV at an angle of photons’ incidence on the sample of ~45°, under ultra-high vacuum conditions (2×10^{-10} mbar). In the vicinity of the C*K*-edge, the energy resolution of the monochromator was ~70 meV. The absorption spectra were normalized to the incident photon flux by measuring the total electron yield from the clean gold crystal surface mounted on the manipulator. The absorption spectra were calibrated by measuring the C*K*-spectra of C_{60} crystals near the position of the C1$s\rightarrow\pi^*$(C=C) resonance at 284.5 eV.

The EXAFS spectra near the Fe K edge (7100 eV) of Fe trace impurities in CD_x films were measured at the EXAFS Beamline (energy range 4.5–31 keV with Si(111) monochromator) of the Siberian Synchrotron Radiation Center at the VEPP-3 source [11]. The spectra were measured in the fluorescent mode and were processed by conventional methods.

Results and discussion

C1s NEXAFS spectra

As seen in NEXAFS pattern of CD_x flake (Fig. 2), the following features are observed in the pre-edge region, that is below the ionization threshold near 290 eV (see the line "Ionization Potential" in Fig. 1), corresponding to the C1*s* → π^* transitions: the resonance peak at 285.0 eV, the inflection points at 287.0 eV, 287.7 eV and the peak at 288.5 eV. The resonance at 285.0 eV corresponds to the transition into the sp^2 states C1*s* → π^* (C = C). The inflection point near 287.0 eV corresponds to the C1*s* → π^* (C=O) transition involving oxygen, which is present in CD_x films in an amount of 8–9 at.%, according to XPS measurements [7].

In the publications on *a*-C:H polymer films, it is identified as a peak of ~286.8 eV – for oxygen in the near-surface region of the film, according to Lenardi [12], or in the region of 286.4 eV – for nanostructured (cluster) films of *a*-C:H with the presence of oxygen, mainly on the cluster border, according to Jaouen [13]. The inflection point at 287.7 eV is a Rydberg resonance (C – H)* with the participation of sp^3 (C – H) bonds. This feature was observed in the works on *a*-C:H and *a*-C films in the energy range 287.5 – 288.0 eV [14–16], as well as in the spectra of polymer films – polyethylene and polystyrene in the region of 287.7 – 288.2 eV, where it is also attributed to Rydberg transitions (before the ionization threshold) for saturated hydrocarbons [17]. A similar shoulder near 287.5 eV for (C – H)* resonance is also observed in complex alcohols with C–C bonds, which are attributed to the C–CH_3 and C–CH_2 end groups in propanol [18]. The last of the observed peaks at 288.5 eV in the pre-edge region is referred to exciton processes in disordered C sp^3 systems (*a*-C films), with a high localization of excited states as a result of disordering, in the energy range of 288.5–288.7 eV [12, 16, 19]. At the same time, the addition of this peak to the C1*s* → π* (O = C – OH) transition at 288.5 eV, suggested in [13] for amorphous *a*-C:H films obtained by ionic Ar + H_2 graphite sputtering. In this case, it also includes oxygen impurity (~8 at.%) and the presence of Fe, Cr (< 3 and 2 at.%, respectively) due to sputtering the walls of the chamber. Also, according to Ray [20], the peak near 288.6 eV (for Fe ~11 at.%), is attributed to the C2*p* – Fe3*d* hybridization and possible C–O bond contributions. However, the C2*p* – Fe3*d* hybridization in these works is not the case for CD_x films with a low Fe impurity content ~0.7 at.%, as was shown earlier [5]. Also, the authors of works [5] and [16] ascertained that a doped iron (<1 at.%) atom in *a*-C:H films is surrounded by five C atoms (as in ferrocene) and such atoms are uniformly distributed without interaction with each other. Indeed, in amorphous *a*-C: H films with relative concentrations of trace metals *Me* ~ 1 at.%, a relatively uniform dissolution in an amorphous carbon matrix was usually observed, the authors of work [5], and with increasing concentration, metals can form either *Me*-nanoclusters (especially, in case of non-transition metals that do not react with carbon) or carbides, under certain conditions.

In the post-threshold region, i.e. above the jump at ~290.7 eV, describing the electronic transitions C1*s* → σ* to the region of unoccupied states, the spectrum has a (C – C)σ* resonance around 292.5 eV, and a broad band at 296–305 eV with a center about 302 eV (C = C)σ* resonance, according to [18, 19]. The far smooth continuum has a broad band at 315–325 eV with a very weakly pronounced maximum of about 320 eV. We did not find an explanation for this at the other works, but the shape of the spectrum in this region shows a certain correlation with the spectrum of condensed n-propanol $CH_3 – CH_2 – CH_2OH$, according to Stöhr [18]. In addition, in [16], a weak and narrower than ours peak at 317–318 eV was reported in *a*-C amorphous films and in diamond films with a predominance of sp^3 hybridization, as well as an even lower intensity of this peak in graphite binding energy, which may be due to the difference in the of C – C bonds' length and the predominant role of sp^3 hybridization [19].

As a result, the $1s \rightarrow \sigma^*$ transitions correspond to the continual group of unoccupied states with three broad asymmetric bands. The observed growth in the width of σ^* resonances with an increase in energy from 292 to 320 eV, is due to a decrease in the lifetime of the final state as a result of an energy growth of the final state.

Finally, in the X-ray absorption spectrum of CD_x films, there are no triple bond resonances $(C\equiv C)\pi^*$ around 285.7–285.9 eV and $(C\equiv C)\sigma^*$ about 308–310 eV [13], which were found, for example, in *a*-C: H films with a low H content, in *a*-C films, and in condensed alcohol groups (propargyl $HC\equiv CH – CH_2OH$) [18]. This is not surprising, since in the studied CD_x films, according to data on FT-IR spectroscopy [2], no C≡C structures were found.

H content and sp^2/sp^3 ratio

Finally, following the empirical dependence from Buijnsters [15] on the relation of the relative hydrogen content and the height I~0.48 of the resonance (C – H)* peak at 287.7 eV (Fig. 1), subject to the normalization of the NEXAFS spectrum by 1 and applicable for the H content range [H] = (25–50) at.%:

$$[H] = 20.4 + 39.6\, I(\sigma^* – CH) \quad [at.\%],$$

where [H] = H/(H+C), we obtain [H]~39 at.%, or H/C~0.6, which correlates with the previously indicated data for this type of CD_x films with a high D or H content [7]. Besides, a rough estimation was made of the sp^2/sp^3 ratio for measured spectrum of the CD_x film, showed: sp^3 ~ 0.63, sp^2 ~ 0.37. The obtained values turned out to be rather close to measurements using X-ray Auger spectroscopy and X-ray photoelectron spectroscopy for such type of films [2, 5, 7] which showed the proportion of sp^3 states ~ 60–70% in CD_x flakes. Also, the EPR narrow line [5] showed a value of $g \geq 2.003$, which indicates a significant sp^3 ratio.

In general, this CD_x spectrum is typical for NEXAFS spectra of K-shells of $sp^3 + sp^2$ hydrocarbon systems having three typical resonance regions: the first π^* resonance in the 285 ± 1 eV region, C–H* resonances in the 288 ± 1 eV region and the broad feature of σ^* resonances between 290 and 315 eV [18].

Thus, XAS results are consistent with the fractal (self-affined) model [2] obtained by various experimental methods, that describes a branched and highly cross-linked 3-dimentional carbon sp^3+sp^2 network with a high hydrogen ratio, i.e., accumulating a large number of H-isotopes and hydrocarbons. Namely, the fractals are of typical size of ~1–60 nm, starting from primary sp^2 particles, consisting of three benzene rings, a minimal fractal aggregate with a size of ~2–3 nm, and different type binding linear elements, i.e. linear sp^3 structural elements like C–C, C–H(D), $C–D_{2,3}$, C–O, O–H, $C_xD(H)_y$, etc., and linear sp^2 C=C, C=O elements [2], where oxygen impurity in the surface layer is adsorbed from atmosphere.

Fe K-edge EXAFS spectra of Fe impurities

Fig. 3(a-c) shows the EXAFS spectra for the Fe *K*-edge (7100 eV) of Fe impurities found in CD_x films with a relative concentration of ~0.7 at% [5]. The radial distribution function (Fig. 3,c) was calculated from the EXAFS spectra in the form of $\chi(k)k^3$ as a modulus of the Fourier transform in the inverse wavelength range of 3.5–10.2 $Å^{-1}$ (Fig. 3,b). The spectra were fitted using the EXCURV92 software [21]. The Debye–Waller factors were fixed and equal to 0.005 $Å^2$. The curves $\chi(k)k^3$ and radial distribution functions, describing the local environment of iron, are shown in Figs. 3,b and 3,c. The fitting procedure gives the following values: the Fe–C distance is 2.11 Å (±1%) (typical C–H (D) distances are ~1.45 Å), and the corresponding coordination number is 6.2 (±10%). Thus, Fe cations occupy mainly octahedral positions in the environment of C atoms, and any features of far Fe–Fe coordination spheres are absent. Additional analysis shows [5] that since clusters incorporate 0.7 at% of Fe (in the Fe^{3+} state) and are uniformly distributed, the roughly estimated distance between $FeC_{6.2}$-cluster centers is greater than 1.1 nm, i.e., clusters are coupled by magnetic moments, rather than by electron shells, at room temperature.

Important, a comparison with the published EXAFS data demonstrated that the bulk of thick CD_x films has neither Fe_3C carbides, nor iron oxides (α- and γ-Fe_2O_3, FeO, Fe_3O_4) [5], and iron oxides were found in the surface layer.

Thus, Fe ions impurities (in a high spin state S=5/2) form a cluster structure whose interatomic distance Fe–C is 0.211 nm and coordination number is 6.2 (±10%), i.e. close to octahedral, and octahedral coordination is known to be the most common geometry for transition metal complexes. Moreover, we assume that the experimentally obtained Fe coordination number $n = 6.2$ means a certain averaged value for the disordered carbon systems with a fractal structure, when, in addition to impurities with $n = 6$, there may be admixtures with other coordination numbers, like $n = 4$, 5, and, possibly, $n = 8$, as found for Fe-containing minerals [22]. This suggestion is based on the additional analysis of the pre-edge peak and the main XAS peak of the Fe K-edge

EXAFS spectrum for $FeC_{6.2}$ impurity clusters.

Fe-catalysed desorption and hydrogen storage capacity growth

The hydrogen isotopes can be more easily desorbed due to iron impurities (arising from erosion of the chamber walls) reducing the threshold of thermal desorption. The main result of the observed iron catalysis due to iron impurities (<1 at.%) in CD_x films is the shift of the D_2 high-temperature thermal desorption (TD) peak position near 970 K by -24 K, and the increase in the fraction of the weakly bonded adsorption states (at ~750 K peak), i.e., a reduction of desorption barrier for higher Fe content by ~1 at.% caused by Fe3*d* – C2*p* hybridization during heating [6].

To describe this TD peak shift by Fe impurity, a structural cluster model based on the interaction of the Fe^+ ion (S = 5/2) with the 1,3-cyclohexadiene C_6H_8 molecule was proposed using *ab initio* methods of quantum chemistry [6], and it was established the reduction of the TD activation desorption barrier for H_2 by about 1 eV. The model 1,3-C_6H_8 molecule has carbon atoms which are six-fold coordinated to the Fe ion, and this molecule was selected based on the fractal model of CD_x films [2].

Besides, highly dispersed metal catalyst nanoparticles as impurities, about 1 nm in size and non-interacting with carbon chemically (present as impurities in CD_x films), are known to increase the carbon hydrogen storage capacity by several times even at room temperature, since it will increase metal surface area for effective dissociation of H_2 molecules to facilitate the transport of dissociated hydrogen in a carbon matrix, according to Xia [23]. Though, this effect was not considered experimentally for CD_x films.

Conclusions

The recorded C *K*-spectra of amorphous CD_x ($x \sim 0.5$) films were found typical for *C* 1*s* spectra of sp^3+sp^2 hydrocarbon systems with a high H/C ratio. In our case, H/C is ~0.6 and the sp^2/sp^3 ratio equals to 0.37/0.63 without admixture of carbyne sp^1 phase. This agrees with a fractal structure of CD_x films forming a branched and highly cross-linked 3*D* carbon sp^3+sp^2 network with a high sp^3 ratio, or matrix, accumulating a large number of H-isotopes and C_xH_y hydrocarbons, all of which can be effused at different temperatures during thermal desorption.

Besides, the D_2 thermal desorption curve of CD_x films appeared to be comparable to that of a nanostructured graphite powder. This TD resemblance together with the observed similarities in XRD and Raman spectra shows the similarities in the TD processes occurring in both carbon systems within the given temperature range 400 – 1000 K and for minimal structural sp^2 elements below 4 nm in nanostructured graphite, which are rather close in size to the minimal sp^2 fractal aggregate ~2–3 nm in the fractal model of CD_x films.

The hydrogen sorption capacity of CD_x films can be increased by several times due to additional porosity growth under moderate heating up to ~600 K. The impurity Fe ions (0.7 at.%), found in CD_x films from the Fe *K*-edge spectra, form a cluster structure close to octahedral with $d_{Fe–C}$ ~0.211 nm and n=6.2±10%.

As it was found out from our experiments and confirmed by our simulations, the H storage and thermal desorption properties of these unique films can be improved by their inherent Fe impurities, capable to reduce the barrier of TD and to increase the C/H storage capacity by several times even at room temperature.

All these properties will contribute to the energy storage applications of these hydrocarbon systems.

Acknowledgements

The authors thank B.N. Kolbasov and L.N. Khimchenko (RNC Kurchatov Insitute, Russia) for providing the CD_x samples. The authors thank Helmholtz–Zentrum Berlin (Germany) for the allocation of synchrotron radiation beamtime. This research project was supported by the Russian-German Laboratory at BESSY II.

Declaration of interest statement

None.

References

[1] Atsumi, H.; Tauchi, K. Hydrogen Absorption and Transport in Graphite Materials. *J. Alloys Comp.,* **2003**, *356–357,* 705–709.

[2] Svechnikov, N. Yu.; Stankevich, V. G.; Kolbasov, B. N.; Zubavichus, Y. V.; Veligzhanin, A. A.; Somenkov, V. A.; Sukhanov, L. P.; Lebedev, A. M.; Menshikov, K.A. Cluster-type Structure of Amorphous Smooth Hydrocarbon CD_x Films ($x \sim 0.5$) from T-10 Tokamak. *J. Surf. Invest.: X-ray, Synchrotron Neutron Tech.,* **2017**, *11*, 1208.

[3] Svechnikov, N.Yu.; Stankevich, V.G.; Sukhanov, L.P.; Menshikov, K.A.; Lebedev, A.M.; Kolbasov, B.N.; Zubavichus, Y.V.; Rajarathnam, D. Investigations of Adsorption States of Protium and Deuterium in Redeposited Carbon Flakes Formed in Tokamak T-10. *J. Nucl. Mater*, **2008**, *376*, 152–159.

[4] Orimo, S.; Matsushima, T.; Fujii, H.; Fukunaga, T.; Majer, G. Hydrogen Desorption Property of Mechanically Prepared Nanostructured Graphite. *J. Appl. Phys.*, **2001**, *90*, 1545-1549.

[5] Svechnikov, N. Yu.; Stankevich, V. G.; Sukhanov, L. P.; Lebedev, A. M.; Menshikov, K. A. Detection of the Iron Impurity in CD_x Films Formed in the T-10

Tokamak and its Influence on the $sp^3 \rightarrow sp^2$ Conversion. *J. Surf. Invest.: X-ray, Synchrotron Neutron Tech.,* **2015**, *9*, 1221–1227.

[6] Stankevich, V. G.; Sukhanov, L. P.; Svechnikov, N. Yu.; Lebedev, A. M.; Menshikov, K. A.; Kolbasov, B. N. Experimental and Theoretical Investigation of Fe-catalysis Phenomenon in Hydrogen Thermal Desorption from Hydrocarbon Plasma-discharge Films from T-10 Tokamak. *Eur. Phys. J. Appl. Phys.,* **2017**, *80*, 20301.

[7] Svechnikov, N. Yu.; Stankevich, V. G.; Arkhipov, I. I.; Grashin, S. A.; Maslakov, K. I.; Lebedev, A. M.; Sukhanov, L. P.; Menshikov, K. A.; Martinenko, Yu. V. Electron Structure Investigations of Homogeneous Hydrocarbon Films Formed in Plasma Conditions of T-10 tokamak. *J. Surf. Invest.: X-ray, Synchrotron Neutron Tech.,* **2013**, *7*, 863–869.

[8] Svechnikov, N.Yu.; Stankevich, V.G.; Lebedev, A.M.; Menshikov, K.A.; Kolbasov, B.N.; Guseva, M.I.; Khimchenko, L.N.; Rajarathnam, D.; Kostetsky, Yu.Yu. Temperature and Spectroscopic Characteristics of Homogeneous Co-deposited Carbon/Deuterium Films from the T-10 Tokamak. *Plasma Devices Oper*, **2006**, *14*, 137–157.

[9] Yin, Y.; Collins, R.E.; Zhang, Q-C. Formation of Porosity in Sputtered Amorphous Hydrogenated Carbon Films. *J. Mater. Science*, **1994**, *29*, 5794–5800.

[10] Molodtsov, S. L.; Fedoseenko, S. I.; Vyalikh, D. V.; Iossifov, I. E.; Follath, R.; Gorovikov, S. A.; Brzhezinskaya, M. M.; Dedkov, Yu. S.; Puettner, R.; Schmidt, J.-S.; et al. High-Resolution Russian-German Beamline at BESSY. *Appl. Phys. A*, **2009**, *94*, 501-505.

[11] Kochubey, D.I. *EXAFS Spectroscopy of Catalysts*; Nauka: Novosibirsk, 1992.

[12] Lenardi, C.; Piseri, P.; Briois, V.; Bottani, C. E.; Bassi, A. Li; Milani, P. Near-edge X-ray Absorption Fine Structure and Raman Characterization of Amorphous and Nanostructured Carbon Films. *J. Appl. Phys.*, **1999**, *85*, 7159–7167.

[13] Jaouen, M.; Tourillon, G.; Delafond, J.; Junqua, N.; Hug, G. A NEXAFS Characterization of Ion-Beam-Assisted Carbon-Sputtered Thin Films. *Diamond Rel. Mater.*, **1995**, *4*, 200 – 206.

[14] Chen, J.G. NEXAFS Investigations of Transition Metal Oxides, Nitrides, Carbides, Sulfides and Other Interstitial Compounds. *Surf. Sci. Rep.*, **1977**, *30*, 1–152.

[15] Buijnsters, J. G.; Gago, R.; Jiménez, I.; Camero, M.; Agulló-Rueda, F.; Gómez-Aleixandre, C. Hydrogen Quantification in Hydrogenated Amorphous Carbon Films by Infrared, Raman, and X-ray Absorption Near Edge Spectroscopies. *J. Appl. Phys.*. **2009**, *105*, 093510.

[16] Gutie´rrez, A.; Dı´az, J.; Lopez, M. F. X-ray Absorption Spectroscopy Study of Pulsed-Laser-Evaporated Amorphous Carbon Films. *Appl. Phys. A*, **1995**, *61*, 111.

[17] Przybylski, M.; Stamm, M.; Zietz, R. Soft X-ray Irradiation Effects in Polymer Films. *J. Physique*, **1987**, *48*, 1351–1356.

[18] Stöhr, J. *NEXAFS Spectroscopy* ; Springer Verlag: Berlin-Heidelberg-New York, 1996.

[19] Gutiérrez, A.; López, M.F. First Experimental Evidence of a C 1s Core Exciton in Amorphous Carbon Films. *Europhys. Lett.*, **1995**, *31*, 299 –303.

[20] Ray, S. C.; Pong, W. F.; Papakonstantinou**,** P. Iron, Nitrogen and Silicon Doped Diamond Like Carbon (DLC) Thin Films: A Comparative Study. *Thin Solid Films,* **2016**, *610*, 42– 47.

[21] Binsted, N.; Campbell, J.V.; Gurman, S. J.; Stephenson, P.C. EXCURV92 Program. SERC Daresbury Laboratory, UK, 1991.

[22] Choi, S.H.; Wood, B.R.; Bell, A.T.; Janicke, M.T.; Ott, K.C. X-ray Absorption Fine Structure Analysis of the Local Environment of Fe in Fe/Al-MFI. *J. Phys. Chem. B*, **2004**, *108*, 8970-8975.

[23] Xia, Y.; Yang, Z.; Zhu**,** Y. Porous Carbon-based Materials for Hydrogen Storage: Advancement and Challenges**.** *J. Mater. Chem. A*, **2013**, *1*, 9365– 9381.

Figure 1. Photo image (left) and scanning electron microscopy image (right) of free standing CD_x films (“flakes“).

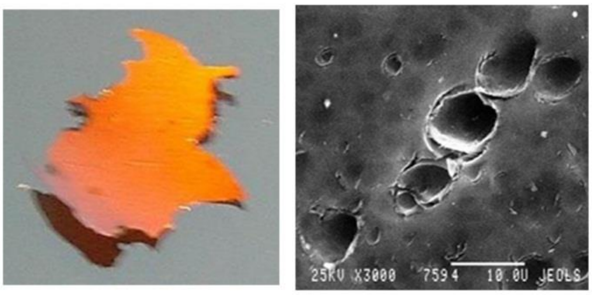

Figure 2. C1*s* NEXAFS spectrum of a typical CD_x film ($x \sim 0.5$).

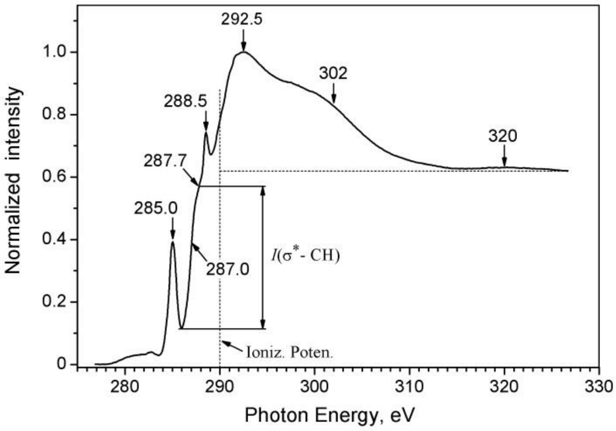

Figure 3. Fe *K*-edge EXAFS spectrum of Fe trace impurities in CD_x films.

(a) Normalized Fe *K*-edge EXAFS spectrum of Fe impurities (noise is filtered out); (b) fitting of the EXAFS spectra by the function $\chi(k)k^3$, where $\chi(k)$ is the EXAFS signal and k is the wave vector ($Å^{-1}$); and (c) the radial distribution function (the Fourier transform amplitude and distance (in Å). The solid and dotted lines show the experimental and calculated results, respectively.

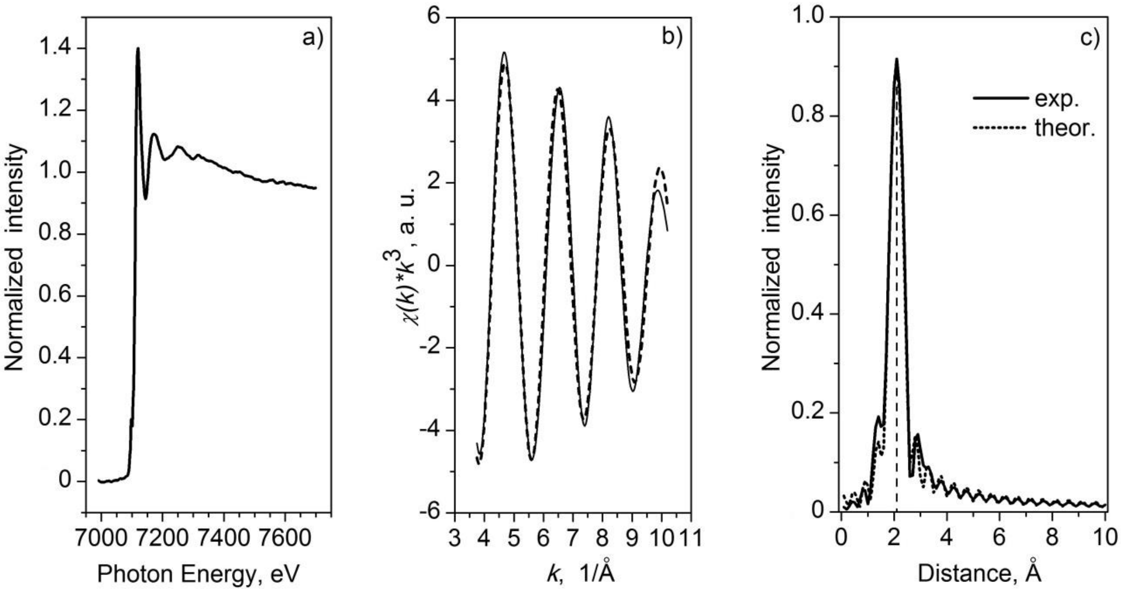

Figure captions

Figure 1. Photo image (left) and scanning electron microscopy image (right) of free standing CD_x films (“flakes“).

Figure 2. C1*s* NEXAFS spectrum of a typical CD_x film ($x \sim 0.5$).

Figure 3. Fe *K*-edge EXAFS spectrum of Fe trace impurities in CD_x films.

(a) Normalized Fe *K*-edge EXAFS spectrum of Fe impurities (noise is filtered out); (b) fitting of the EXAFS spectra by the function $\chi(k)k^3$, where $\chi(k)$ is the EXAFS signal and k is the wave vector (Å^{-1}); and (c) the radial distribution function (the Fourier transform amplitude and distance (in Å). The solid and dotted lines show the experimental and calculated results, respectively.